Testing of Soft Regolith Dynamic Anchors for Celestial Exploration

T. Ebert[1,2] and P. Larochelle[2]

[1]Granular Mechanics and Regolith Operations Laboratory, National Aeronautics and Space Administration. Kennedy Space Center, FL 32899; email: tom.ebert-1@nasa.gov
[2]Robotic and Spatial Systems Laboratory, Department of Mechanical and Aerospace Engineering, Florida Institute of Technology, Melbourne, FL 32901; email: pierrel@fit.edu

ABSTRACT

Recent exploration missions to celestial bodies have shown an increasing demand for surface based landers and rovers designed to perform experiments on the ground, rather than relying purely on traditional orbiting observatories. Many of the scientifically interesting locations have proven hazardous and difficult to reach and traverse, driving the need for different methods of locomotion. Some of these locations lie in deep, permanently shadowed craters or in rocky, highly uneven landscapes. Various wheeled, flying, jumping and legged rovers have been proposed, some of which have been implemented with success and problems alike. The presented work focuses on a category of legged rovers intended to climb up steep slopes covered in soft soil or regolith, such as those found on crater walls on the moon and Mars. The envisioned rover would utilized dynamic anchors on the feet of its legs to claw into the surface, engaging and disengaging with each step. This clawing effect can also be used to anchor a lander in near zero gravity on a comet or asteroid. A method for evaluating the performance of different dynamic anchors is proposed and implemented. Physical testing is performed by using a robotic arm to engage a series of anchors with a lunar regolith simulant while measuring the engagement, holding, and disengagement forces. A range of anchor geometries and engagement angles is evaluated and the results are analyzed to determine which parameters effect the holding force and in which way.

INTRODUCTION

During the first several decades of space exploration, missions have primarily employed spacecraft designed to perform science from a distance. Celestial exploration has traditionally been performed from the safety of an orbital patch around the planet, moon, comet, or asteroid of interest. Missions of this type are still gathering scientific data very successfully, notably the New Horizons mission that recently reached Pluto, capturing never before details of dwarf planet's surface and its moons, as described by Dunbar (2015). As we prepare to move humanity deeper into space it is becoming increasingly more important to gather data on available resources on-site to determine what can be used locally and what must be brought along from earth. This requires robotic landers to land on the celestial bodies' surface,

and frequently move to different locations once touchdown is completed. Many of these surface mission have gone to Mars, including the stationary Phoenix Lander, which found water ice a few centimeters below the polar soil according to Watanabe (2015), as well as the Curiosity rover, which has been slowly been climbing the foothills of Mount Sharp, as described by Anderson (2015).

One unconventional surface mission was LCROSS, described by Andrews (2010), in which a spent upper rocket stage was guided to a targeted crash impact inside a crater on the Moon. That mission yielded substantial evidence of water ice at the bottom of permanently shadows craters, where the ice brought there by comet is not sublimated by the suns heat. Unfortunately it is hard to reach the bottom of such craters with conventional landers. This also applies to many other scientifically interesting locations, such as the steep slopes of Mount Sharpe, or the Icy moons of Jupiter.

The research presented here aims to support a new type of mobile surface explorer capable of traversing much more difficult terrain than conventional rovers. The anchors evaluated here are envisioned to be used as a claw on each foot of four or more legged walking robot. These claws would grab the loose soil found on the moon and Mars to climb steep slopes, or hold on to the surface in low gravity environments such as asteroids. One example of a walking robot that could benefit from such anchoring claws is Spot presented by Ackerman (2015), the latest iteration of Boston Dynamics four legged platform, which is already capable of walking up and down impressive slopes on hardened surfaces. Spot is shown in Figure 1.

Dynamic anchoring in this paper refers to the ability to engage and disengage each anchor repeatedly to allow for the continuous locomotion along soft terrain. The anchor holding force is of primary interest to evaluate the performance of each anchor. In this case, the holding force is not defined as the anchor or holding capacity, but rather the force parallel to the surface which is being traversed. Only the force vector parallel to surface is considers due to the assumption that the robot will have a low center of gravity to minimize the pull-out angle deviation from the surface. Additionally, the engagement and disengagement forces perpendicular to the surface are important, particular in the low gravity application where too much engagement force could push the robot off an asteroid's surface, or available disengagement force could allow the robot to remain attached to the asteroid's surface. It is assumed that the robot leg design functions in such a way that the perpendicular force is generated independently from the holding force. These assumption varies drastically from those utilized in the standard drag embedment anchor mechanics analysis, such as that presented by Aubeny and Chi (2010). The forces were recorded during testing on several different anchor geometries. The evaluated anchors are simplified geometries, the actual anchoring mechanism designs are left for future research. The testing results are compared for each anchor to determine which anchor variables most affect the associated forces. The study of the effect of different regolith is not included in the research, only the effect of varying anchor properties. The presented results would vary given different types of simulant or regolith.

Figure 1. Spot by Boston Dynamics (Ackerman (2015))

RELATED RESEARCH

Dynamic Anchoring has been studied in several previous research projects. SpinyBot, developed by Asbeck et al (2006) at Stanford University, is a six legged gecko-like robot that uses micro spines, or tiny flexible hooks, on the bottom of its feet to engage rough surface features on stone, brick, or stucco walls. The rough features can be on a microscopic scale but cannot exceed a certain size relative to the body of the robot. Asbeck (2010) also developed StickyBot, a similar gecko inspired robot that uses four legs and directional adhesives to climb up smooth surfaces such as glass. Both of these robots are mobility platforms capable of climbing vertical surfaces without a tether, but rely on hard surfaces to function properly. Alternatively, AXEL, developed at NASA's Jet Propulsion Laboratory by Abad-Manterola et al (2009) is a two-wheeled tail dragging platform that can anchor at the top of a slope and repel down on a tether. The large wheels allow it to swing side to side while on near vertical slopes made up of a wide variety of materials and surface features. However, the tether limits its range and is susceptible to snagging. AXEL is capable of anchoring in soft soil, but the anchor is engaged and then used to hold the tether statically at the top of a slope. Marvi et al. (2014) at Georgia Institute of Technology evaluated the effectiveness of the snake robot developed at Carnegie Mellon University in emulating the side winding locomotion of a rattle snake on slopes of sand dunes. They showed efficient, near slip-less locomotion in very soft sand, however, the nature of the design requires a very low profile robot.

Despite extensive research into analytical prediction in the sub-discipline of anchor mechanics, as summarized and extended upon by Aubeny and Chi (2010), there is still a large reliance on scale model testing and empirical methods such as the work presented in this paper. A comprehensive summary of empirical methods and results is presented by the Naval Civil Engineering Laboratory (1987) in their work on naval

drag anchors. Due to the application on ship anchors, however, the studied soil types do not include materials similar to soft, dry regolith. Additionally such studies typically assume the anchor line applies a vertically upward component to the anchor, which is not applicable to the dynamic anchor presented here.

Research has also been performed to study the interaction between rover wheels and soft regolith in the field of terramechanics, such as the work presented by Scharringhausen et al. (2009) and Richter et al. (2006), who presented a predictive wheel interaction model based on actual data from Mars Rovers, as well as Iagnemma et al. (2011), who developed a new interaction model specifically for Mars Rovers for use in simulations. These studies are usually limited to a small the interaction depth to tool size ratio due to the requirement that the wheels not sink far into the regolith. Therefore, deep penetration are not of interest in such studies

Several studies related to tool-regolith interaction have been performed, primarily with the application of excavating regolith for further use. One such study, which includes a test apparatus for determining failure forces was presented by Willman and Boles (1995). They apply multiple previously developed predictive models for excavation forces to a specific lunar simulant using its properties, and then compare the results to actual data obtained from testing. Their research however, only varies the depth, and does not alter the geometry of the excavating tool.

TEST SETUP

The test setup utilized to evaluate the various anchors consists of an instrumented bin filled with BP-1, a lunar regolith simulant, and the geometric representations of each anchor attached to a robotic arm. The BP-1, which stands for Black Point 1, is named after the location at which it was found. It is a mining byproduct that is has been shown to have nearly identical properties to other high fidelity simulants by Rahmatian and Metzger (2010), and much less expensive than the artificially produced JSC-1A. It was decided to use this BP-1 as a representative material for soft regolith that can be expected to be found on a target celestial body. BP-1 in particular represents the expected properties, including grain size distribution for the lunar surface.

The test bin is an open, 20cm tall, 50cm square container mounted on low friction, four large diameter wheels. These wheels allow the bin to deflect a horizontally oriented load-cell to measure the anchoring force. The bin can also be reconfigured to measure the engagement and disengagement forces by supporting the common axis of two wheels with a vertically oriented load-cell. Photos of these configurations are shown in Figure 2 and a schematic of both configurations is depicted in Figure 3, where the horizontal measurement location is denoted with an “H” and the vertical measurement location with a “V”.

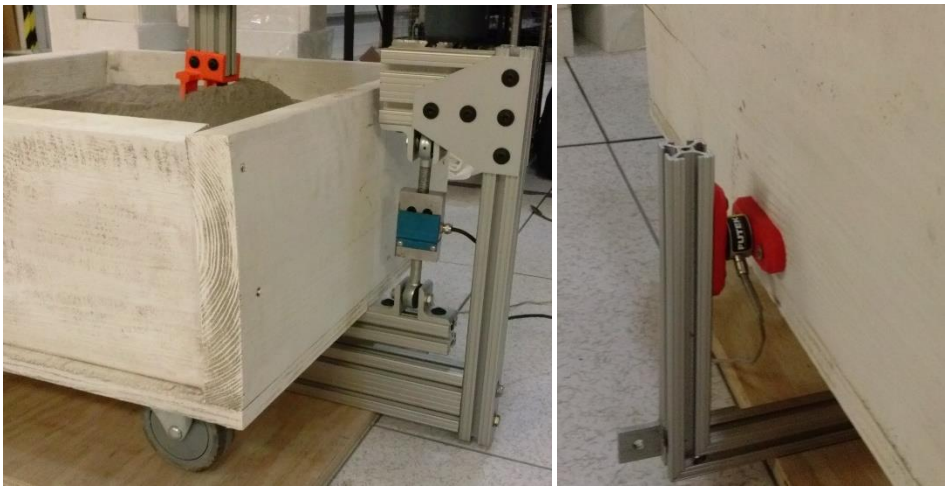

Figure 2. Load-cell Setup: Vertical (left) and Horizontal (right)

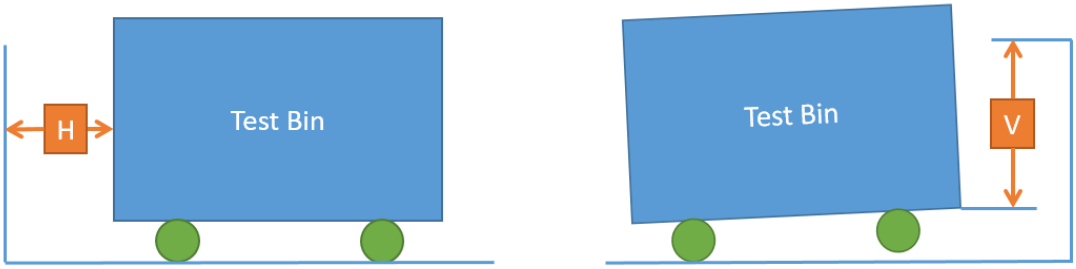

Figure 3. Test Setup: Horizontal (left) and Vertical (right)

The vertical force requires a moment arm conversion since the test bin is pivoting about the common axis of the wheels that remain in contact with the ground. This moment arm conversion is held constant because the bin is rotated 90 degrees during the vertical measurements, making the anchor drag direction parallel to this pivot axis. The bin is filled to within 4 cm of the top edge with BP-1, resulting in a total simulant height of 16 cm.

The anchors tested in this research are simple geometries chosen to get a broad spectrum of possible anchoring mechanism designs. Features are also incorporated that allow for minor modifications to evaluate the sensitivity of the anchoring forces to variables such as anchor mounting angle, number of protrusions, and protrusion arrangement.. In all, six unique anchor geometries were tested. A flat plate anchor, 6.5 cm wide by 10 cm tall by 2 mm thick with a 60 degree chamfered tip is shown on the right in Figure 4. The plate is stiffened by a set of two tapered gussets on the back side. A single spike anchor consist of a V shaped cross-section that is extruded vertically to a length of 10 cm. The V shape has a 90 degree angle, and is 2 cm wide. A double spike anchor has two of these spikes side by side, with a 2 cm gap between them. The double spike anchor is shown on the left in Figure 4. Lastly, a family of rod anchors consists of one or more 6 mm diameter rods that protrude 10 cm vertically from a mounting plate. Three different rod combinations were tested; a

single center rod, three rods side by side with a 2 cm spacing between them, and an eight rod configuration with two rows of 4 side by side rods with a 1.5 cm spacing. The eight rod configuration is shown in in the center of Figure 4. A fully populated 11 rod configuration, combining the three rod and the eight rod setups, was also attempted, but the anchoring forces exceeded the test setup capabilities. All of these anchors were additively manufactured on a MakerBot Replicator 2 with PLA filament. Each one has a common mounting feature that allows it to be mounted to the robot arm end effector.

Figure 4. Double Spike (left), Eight Rod (center), and Flat Plate (right)

The robot arm used to generate the anchoring motion profile is a Fanuc M-410iC, a 4 degree of freedom robot arm, in which the end-effector is always parallel to the ground. Its payload capacity is significantly above the forces applied by the anchors, therefore the programmed motion profile is identical for each test run. Three separate motion profiles were used throughout the testing, one pure vertical, and two at opposing 10 degree angles off vertical. The vertical profile inserts each tool 5 cm into the BP-1 straight down, pulls horizontally for 20cm, then extracts the tool straight up completely out of the BP-1. The other two profiles each insert the tool into the BP-1 following a 10 degree path tilted towards or away from the pull direction. The remainder of these two profiles are identical to the vertical profile. Each profile ensure that a minimum 10 cm clearance is maintained to the bottom and side walls of the test bin.

The data from each of the two load-cells is recorded using a National Instruments compact data acquisition card called up by a custom LabVIEW program. Only the teach pendant is available to run the Fanuc robot, so timing integration between the software and the robot arm is manual. Two half second hold points are programmed into the robot path as visual trigger to start and stop the recording within the LabVIEW program, which still allows for slight differences in start and stop times for each recording. The raw data is recorded at 100 Hz which is affected by some oscillation caused by the motion of the large robot arm. This oscillation is mitigated mechanically by partially isolating the test bin from the floor and in software by applying a moving average.

RESULTS

In order to generate a meaningful array of test cases, each anchor is tested at the aforementioned pure vertical as well as at 10 degrees forward and backward tilt angles. In addition, the plate anchor and double spike anchor are tested while rotated 180 degrees about the vertical axis as they have unique features that are believed to affect the forces involved. This results in a total of twenty individual test configurations, all of which are summarized in the first column of Table 1.

The many variables governing the behavior of the anchors within the regolith required special treatment to enable the gathering of comparable data. The consistent path taken by the robot was mentioned paragraph 3 of the Test Setup section. Each tool is moved along the path a total of seven times. Since the regolith is assumed to be loose and uncompressed in the scope of this research, each anchor is first dragged though the simulant bin along the respective path to loosen up the affected area. The displaced regolith is placed back into the excavated area by gently brushing the surrounding material. Figure 5 shows examples of the excavated area for multiple anchor configurations. Next, five identical test runs are performed, with the regolith reset as described above before each run. The final test run is performed without resetting the simulant, following in the previously excavated area. This run is included to examine what would happen if a hind leg steps into the footprint of a front leg on the hypothetical exploration robot.

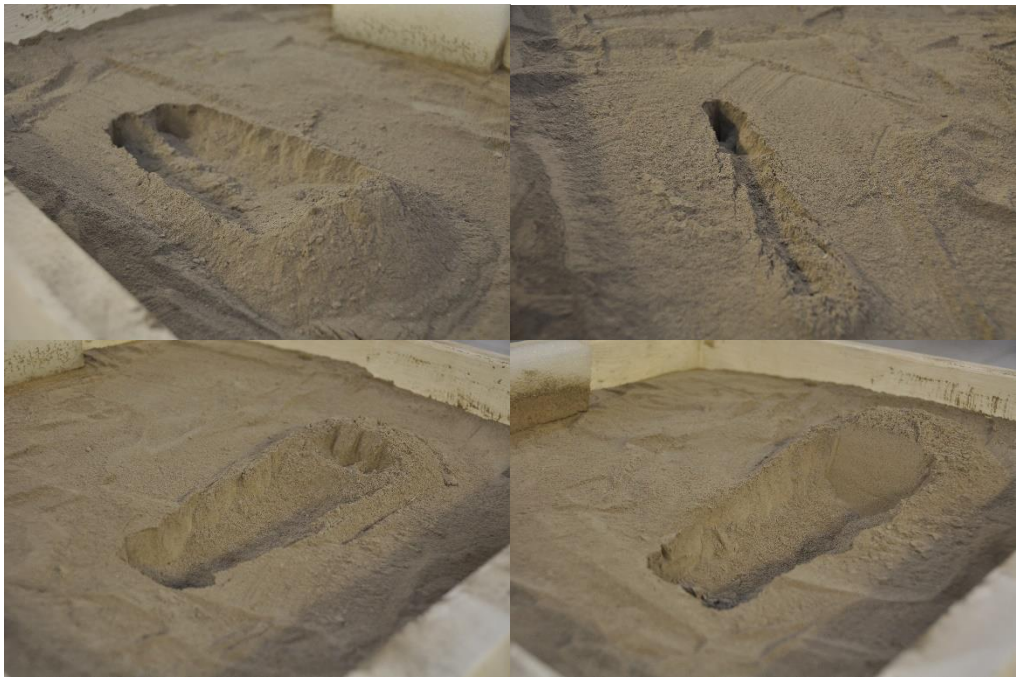

Figure 5. Excavated Profiles: Double Spike (top-left), One Rod (top-right), Three Rod (bottom-left), and Flat Plate (bottom-right)

For the horizontal direction the peak force is what is available to use for the anchoring of an exploration robot. Similarly, the vertical force peak is what must be reacted to be able to insert each anchored foot. Both peak numbers are extracted directly from the smoothed data. The average of the five peak forces for each

anchor's test is shown in Table 1 along with the peak force from the run that follows the previously excavated path.

Table 1. Summary of Peak Forces for all 20 Anchor Configurations

Anchor Configuration	*Forces in Newtons (Average of 5 Runs)*		*Forces in Newtons (Non-Reset Run)*	
	Horizontal	*Vertical*	*Horizontal*	*Vertical*
One Rod, 0°	25.4	4.1	25.4	5.4
Three Rod, 0°	80.0	11.6	76.5	10.2
Three Rod, 10°	61.0	11.6	61.4	6.8
Three Rod, -10°	75.9	20.9	73.4	14.4
Eight Rod, 0°	166.4	75.1	129.0	30.6
Plate, 0°	108.5	39.6	77.8	30.6
Plate, 10°	50.9	11.8	45.8	10.2
Plate, -10°	140.6	54.5	98.8	17.8
Reverse Plate, 0°	130.5	45.2	97.9	28.9
Reverse Plate, 10°	101.9	26.8	57.8	22.1
Reverse Plate, -10°	87.6	40.9	71.2	27.2
Single Spike, 0°	34.8	16.5	38.7	15.3
Single Spike, 10°	27.7	8.3	24.0	8.9
Single Spike, -10°	33.0	16.6	31.6	11.0
Double Spike, 0°	74.0	31.1	57.5	26.7
Double Spike, 10°	63.1	16.9	52.9	10.2
Double Spike, -10°	62.9	30.3	59.2	27.6
Rev. Double Spike, 0°	58.1	16.1	26.2	15.3
Rev. Double Spike, 10°	41.4	11.9	25.8	6.8
Rev. Double Spike, -10°	68.8	26.2	55.6	17.4

Data collected during the test runs with the double spike anchor following the vertical path are shown in Figure 6 for the horizontal forces and in Figure 7 for the vertical forces. These graphs are shown as an example of recorded data, similar data was collected for the other 19 configurations. The five solid lines represent the nominal runs with reset regolith, while the dashed line represents the additional run that follows in the excavated path. In both graphs the horizontal axis is time in seconds, and the vertical axis is the force in Newton. A positive value represents a force opposing the direction of anchor travel.

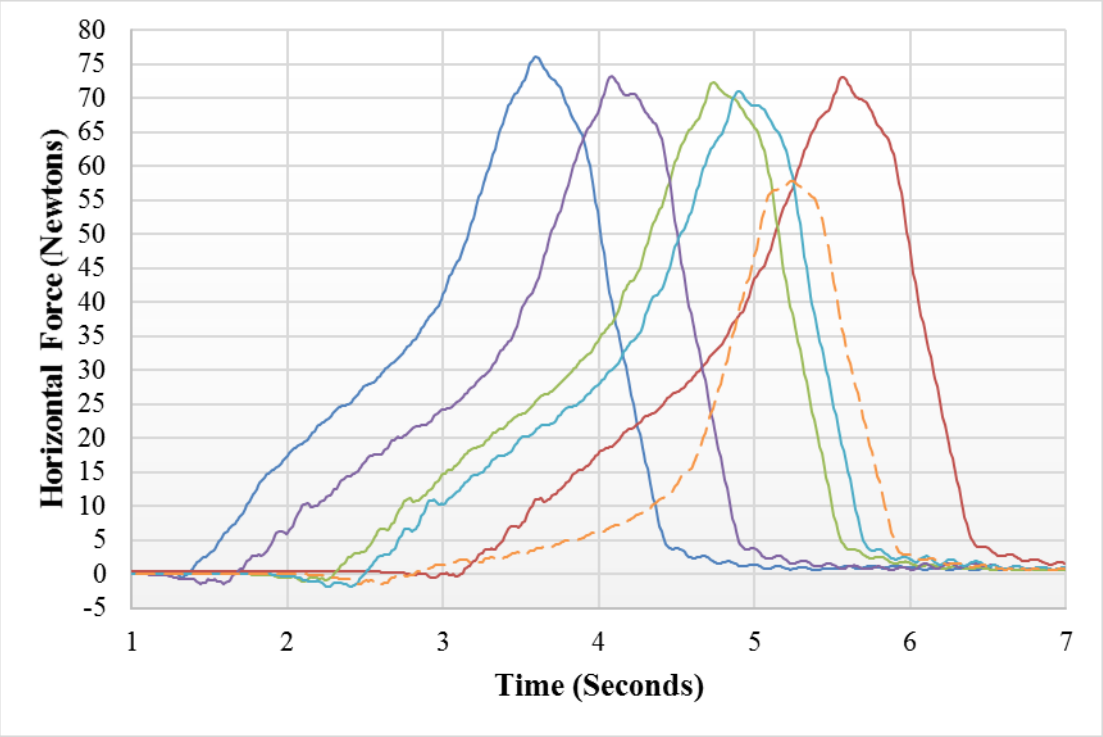

Figure 6. Horizontal Force for Double Spike on Vertical Path

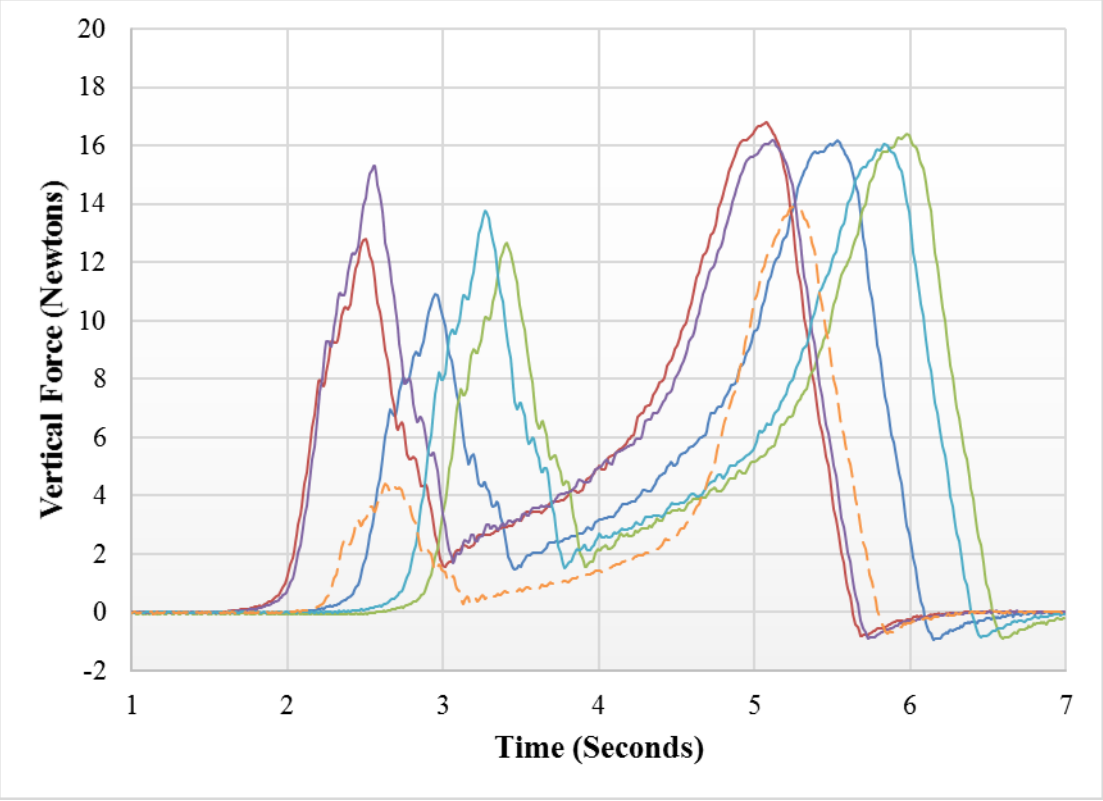

Figure 7. Vertical Force for Double Spike on Vertical Path

CONCLUSION

Several interesting results can be extracted from the recorded test data that lead to conclusions about the factors that influence the associated dynamic anchoring forces. These results are discussed in detail below, along with future research that can further solidify the conclusions.

Comparing the single spike and the double spike, the measured peak forces are close to twice as large for the double spike across all three anchor angles. The same is true of the one rod versus three rod anchors, where the forces for the vertical path are nearly triple. This proportionality reaches diminishing return for the eight rod anchor, where the forces are only about six and a half times that of the single rod.

The available anchoring force increases as the amount of simulant being displaced increases. However, a comparison between the one rod and three rod anchors shows more than three times the displaced regolith, meaning the force is not directly proportional.

The anchors with the higher horizontal forces also have a much smaller vertical to horizontal force ratio, which is as little as 2.2, meaning this anchor is less suitable for use in low gravity or steep slope environments where limited reaction force is available to drive and keep the anchor in the regolith. This same ratio is a much more favorable 7 for the three rod anchor while still generating about half the anchoring force of the highest performing anchors.

In general, the 10 degrees forward tilt anchors generated less holding force while the 10 degrees backward tilt generated the same or more holding force as the vertical anchors. This is likely due to the simulant being moved upward out of the way with the forward tilt, while being compressed downward with the backward tilt. The two exceptions to this are the double spike and reverse plate anchors, suggesting that the geometry partially counteracts the compressive nature of the backward tilt.

The reverse double spike and reverse plate show significant difference in holding and engagement force, again suggesting that the specific geometric features affect the way the regolith is displaced and compressed. These features may be able to be exploited to further optimize the anchor geometry.

Examining the forces measured during the runs for which the simulant was not reset, a trend is seen that shows better retained holding forces for the anchors that displace less regolith. As much as 100 percent of the original holding force is available for the smaller anchors such as the one rod, three rod, and single spike configurations. For all anchors a minimum of 45 percent holding force is retained, likely providing a useful anchor point even in the event that the hind leg step into a footprint left by a front leg. It should be noted that the runs that show more than 100 percent of retained holding force are due to the random nature of the regolith, this makes it impossible to provide

identical starting conditions for each run. This randomness has a larger impact on the non-reset data as only one run was performed for each anchor.

Within the tested set of anchor configurations, the one exhibiting the best combination of characteristics appears to be the three rod anchor. It generates a relatively large amount of holding force for the amount of material required and displaced. It also requires the least vertical force relative to the holding force and maintains almost all of its holding force in the event of a previously displaced footprint. Lastly, the three rod anchor is one of the least sensitive to the engagement angle, meaning it can tolerate a bad approach angle of an anchor, which in turn simplifies the leg design and control.

A case study in which a four legged exploration platform utilizing the tested three rod anchor will be performed in future research to further examine the feasibility and capability of such anchors. In particular, the slope ascend capability of such a robot should be computed for a given mass, size, and gravity condition.

REFERENCES

Abad-Manterola, P., Burdick, J. W., Nesnas, I. A. D., and Cecava, J. (2009). "Wheel Design and Tension Analysis for the Tethered AXEL Rover on Extreme Terrain." *Proc., Aerospace Conference*, IEEE, Big Sky, MT.

Ackerman, E (2015), "Spot Is Boston Dynamics' Nimble New Quadruped Robot" *IEEE Spectrum*, <http://spectrum.ieee.org/automaton/robotics/robotics-hardware/spot-is-boston-dynamics-nimble-new-quadruped-robot> (Oct. 10, 2015).

Anderson, R. (2015), "Sol 1112-1113: Rough Driving" *NASA Mars Rover Curiosity: Mission Updates*, <http://mars.nasa.gov/msl/mission/mars-rover-curiosity-mission-updates> (Oct. 2, 2015).

Andrews, D (2010), "Lunar CRater Observation and Sensing Satellite (LCROSS)" *National Aeronautics and Space Administration***,** < http://lcross.arc.nasa.gov/> (Sep. 5, 2015)

Asbeck, A. T. (2010). *Compliant Directional Suspension for Climbing with Spines and Adhesives*. PhD Thesis, Stanford University, Stanford, CA.

Asbeck, A. T., Kim, S., McClung, A., Parness, A., and Cutkosky, M. R. (2006). "Climbing Walls With Microspines." *Proc., International Conference on Robotics & Automation*, IEEE, Orlando, FL.

Aubeny, C. P., Chi, C., (2010). *Mechanics of Drag Embedment Anchors in a Soft Seabed*, Journal of Geotechnical and Geoenvironmental Engineering, ASCE, Vol. 126 No. 1.

Dunbar, B. (2015), "New Horizons", *National Aeronautics and Space Administration***,** <https://www.nasa.gov/mission_pages/newhorizons/main/index.html>, (Oct. 2, 2015)

Marvi, H., Gong, C., Gravish, N., Astley, H., Travers, M., Hatton, R. L., Mendelson III, J. R., Choset, H., Hu, D. L., and Goldman, D. I. (2014), *Sidewinding with*

minimal slip: Snake and robot ascent of sandy slopes, Science Vol. 346 No. 6205.

Naval Civil Engineering Laboratory (NCEL). (1987). "Drag embedment anchors for navy moorings." *Techdata Sheet Rep. No. 83-08R*, NCEL, Port Hueneme, Calif.

Rahmatian, L. A., and Metzger, P.T. (2010), "Soil Test Apparatus for Lunar Surfaces", *Proc., Earth and Space: Engineering, Science, Construction, and Operations in Challenging Environments*, ASCE, Honolulu, HI.

Richter, L., Ellery, A., Gao, Y., Michaud, S., Schmitz, N., and Weiss, S. (2006). *A predictive wheel-soil interaction model for planetary rovers validated in testbeds and against MER Mars rover performance data.* In European Planetary Science Congress, Vol. 1

Scharringhausen, M., Beermann, D., Krömer, O., and Richter, L. (2009), "A wheel-soil interaction model for planetary application." *Proc. 11th European Regional Conference of ISTVS*, Bremen, Germany.

Watanabe, S. (2015), "Phoenix Mars Lander", *National Aeronautics and Space Administration***,** <http://www.jpl.nasa.gov/news/phoenix/main.php>, (Oct. 2, 2015)

Willman, Brian M., and Walter W. Boles (1995), *Soil-tool interaction theories as they apply to lunar soil simulant.* Journal of Aerospace Engineering, Vol. 8, No. 2